Influence of guided acoustic wave Brillouin scattering on excess noise in fiber-based continuous variable quantum key distribution

Yongmin Li,* Ning Wang, Xuyang Wang, and Zengliang Bai

State Key Laboratory of Quantum Optics and Quantum Optics Devices, Institute of Opto-Electronics, Shanxi University, Taiyuan 030006, China
**Corresponding author: yongmin@sxu.edu.cn*

Received June 23, 2014; revised August 18, 2014; accepted August 18, 2014; posted August 19, 2014 (Doc. ID 214626); published September 19, 2014

We experimentally study the depolarized guided acoustic wave Brillouin scattering in a long-distance telecom single-mode fiber (SMF-28e). It is shown that such a scattering process can introduce excess noise and further degrade the performance of the fiber-based continuous variable quantum key distribution (CVQKD) system where a fiber is utilized as the quantum channel. Based on the experimental results we deduce a lower bound for the extinction ratio of the pulsed light in the time-multiplexing CVQKD protocol.

OCIS codes: (270.5568) Quantum cryptography; (190.4370) Nonlinear optics, fibers; (060.5565) Quantum communications.

http://dx.doi.org/10.1364/JOSAB.31.002379

1. INTRODUCTION

Quantum key distribution enables the generation of a random secret key between two valid parties. This ideal was first introduced by Bennett and Brassard in 1984 [1] and is known as the BB84 protocol. Since then, various kinds of protocols have been proposed [2,3]. Among them, continuous variable quantum key distribution (CVQKD) protocols based on quadratures of the quantized electromagnetic field and homodyne or heterodyne detection have seen significant progress during the last decade [4–14].

For CVQKD, the distance for secure communication is determined mainly by the losses of the quantum channel, the excess noises, and the efficiency of data reconciliation. Optical fiber and free space are two main quantum channels used for light fields. Hereafter we focus on the quantum channel in which optical fiber is utilized. Current low-loss telecom single-mode fibers have a lowest loss of ~0.2 dB per kilometer at 1550 nm, which almost reaches the Rayleigh scattering limit. Recently, a breakthrough has also been obtained in reconciliation efficiency with a value of ~95% over a wide range of signal-to-noise ratio [15]. The excess noises that are added by the quantum channel are crucial to the performance of the CVQKD. Even a very small amount of excess noise can deteriorate the secure communication significantly. In CVQKD, two light fields are involved: the signal field and the local oscillator (LO); they are polarization multiplexing and traveling along the same fiber to suppress greatly the relative phase fluctuations between them. The signal field is quite weak and contains up to several tens of photons per pulse usually. However, the LO is relatively intense, and each pulse can involve an average photon number of 10^8. Two possible mechanisms will be responsible for the excess noise associated with the LO. The first issue is photon leakage from the LO into the signal path, which is an important contribution to the excess noise and has been resolved by introducing time multiplexing and polarization multiplexing [6], or polarization and frequency multiplexing [7]. The other one is the nonlinear effect in optical fibers.

Guided acoustic wave Brillouin scattering (GAWBS) [16,17] due to the thermally excited guided acoustic modes of an optical fiber can constitute a significant thermal-noise source to the generation of squeezed lights [18–22]. The vibrational modes mainly responsible for forward scattering are the radial modes R_{0m}, which produce pure phase modulation of light, and the mixed torsional–radial modes TR_{2m}, which change the polarization of light and cause depolarized scattering of light. As mentioned above, the LO and the signal field in CVQKD are polarization multiplexed; thus the depolarized GAWBS can scatter a portion of the LO photons into the signal path inevitably and constitute a thermal-noise source of excess noise. In previous works, the CVQKDs are all implemented in the regime in which relatively long (100 ns) light pulses are utilized; the corresponding frequency bandwidth (Fourier transform limit) is around 10 MHz, which is well below the first TR_{2m} mode (~20 MHz for the telecom single-mode fiber). When one reaches a high-bandwidth secure communication over 1 GHz with a light pulse less than 1 ns, the depolarized GAWBS will be a non-negligible noise source, and one should consider its effect on the performance of secure communication. In this paper, we investigate the effect of depolarized GAWBS in a long-distance telecom single-mode fiber (SMF-28e) on the excess noise in CVQKD. A lower bound for the extinction ratio of the pulsed light in time-multiplexing and polarization-multiplexing CVQKD protocols is deduced, which is necessary to suppress the excess noise coming from the GAWBS.

2. THEORETICAL ANALYSIS

Assume two optical fields, i.e., the signal field and LO, that both propagate in a long-distance (with length of l)

single-mode fiber with orthogonal polarization. Consider the effect of depolarized GAWBS in fiber; the signal field at the fiber output can be described by

$$\hat{a}'_s(t) = \sqrt{1-\eta}\hat{a}_s(t) + \sqrt{\eta}\hat{a}_{\mathrm{LG}}(t), \tag{1}$$

where $\hat{a}_s(t)$ and $\hat{a}'_s(t)$ are signal field at the fiber input and the output signal field from the fiber, respectively. $\hat{a}_{\mathrm{LG}}(t)$ denotes the depolarized GAWBS mode of the LO, and η is the photon scattering efficiency due to the depolarized GAWBS in the fiber. We assume that both the signal field and the LO are optical pulses with duration of T_0; the quadrature of the output signal field can be written as

$$\begin{aligned}\hat{X}'_{s,\theta,\theta'} &= \frac{1}{\sqrt{T_0}}\int_{-T_0/2}^{T_0/2}\left(\sqrt{1-\eta}\hat{X}_{s,\theta}(t) + \sqrt{\eta}\hat{X}_{\mathrm{LG},\theta'}(t)\right)\mathrm{d}t \\ &= \hat{X}_{s,\theta} + \hat{X}_{\mathrm{LG},\theta'},\end{aligned} \tag{2}$$

where the quadrature is defined as $\hat{X}_{s,\theta}(t) = \hat{a}(t)e^{-i\theta} + \hat{a}^{\dagger}(t)e^{i\theta}$, $\hat{X}_{\mathrm{LG},\theta'}(t) = \hat{a}_{\mathrm{LG},\theta'}(t)e^{-i\theta'} + \hat{a}^{\dagger}_{\mathrm{LG},\theta'}(t)e^{i\theta'}$, and θ and θ' are the relative phases between the signal and the LO, and the depolarized GAWBS mode and the LO, respectively. The added excess noise to the signal field due to the depolarized GAWBS can be given by

$$\langle\hat{X}^2_{\mathrm{LG},\theta'}\rangle = \langle\hat{X}'^2_{s,\theta,\theta'}\rangle - \langle\hat{X}^2_{s,\theta}\rangle. \tag{3}$$

To derive the above results we have used the relation of

$$\langle\hat{X}_{s,\theta}\hat{X}_{\mathrm{LG},\theta'}\rangle = \langle\hat{X}_{\mathrm{LG},\theta'}\hat{X}_{s,\theta}\rangle = 0. \tag{4}$$

The quadrature of the output signal field can be expressed in the frequency domain

$$\begin{aligned}\hat{X}'_{s,\theta,\theta'} &= \frac{1}{\sqrt{T_0}}\int_{-T_0/2}^{T_0/2}\hat{X}'_{s,\theta,\theta'}(t)\mathrm{d}t \\ &= \frac{\sqrt{T_0}}{2\pi}\int_{-\infty}^{+\infty}\hat{X}'_{s,\theta,\theta'}(\omega)\mathrm{Sinc}(\omega T_0/2)\mathrm{d}\omega,\end{aligned} \tag{5}$$

where $\hat{X}'_{s,\theta,\theta'}(\omega)$ is the Fourier transform of $\hat{X}'_{s,\theta,\theta'}(t)$.

By using the relation of

$$\langle\hat{X}'_{s,\theta,\theta'}(\omega)\hat{X}'^{\dagger}_{s,\theta,\theta'}(\omega')\rangle = \delta(\omega-\omega')\langle|\hat{X}'_{s,\theta,\theta'}(\omega)|^2\rangle \tag{6}$$

the variance of the quadrature of the output signal field can be represented as

$$\begin{aligned}\langle\hat{X}'^2_{s,\theta,\theta'}\rangle &= \frac{T_0}{(2\pi)^2}\int_{-\infty}^{+\infty}\int_{-\infty}^{+\infty}\langle\hat{X}'_{s,\theta,\theta'}(\omega)\hat{X}'^{\dagger}_{s,\theta,\theta'}(\omega')\rangle \\ &\quad\times\mathrm{Sinc}(\omega T_0/2)\mathrm{Sinc}(\omega' T_0/2)\mathrm{d}\omega\mathrm{d}\omega' \\ &= \frac{T_0}{2\pi}\int_{-\infty}^{+\infty}\langle|\hat{X}'_{s,\theta,\theta'}(\omega)|^2\rangle\mathrm{Sinc}^2(\omega T_0/2)\mathrm{d}\omega.\end{aligned} \tag{7}$$

Because of the dispersion of the long-distance fiber (on the order of several kilometers or longer), we assume that the phase θ' will be random in the range of $[0, 2\pi]$. Under this condition, by using the relation

$$\begin{aligned}\hat{X}'_{s,\theta,\theta'}(\omega) &= \sqrt{1-\eta}(\hat{a}_s(\omega)e^{-i\theta} + \hat{a}_s(-\omega)^{\dagger}e^{i\theta}) \\ &\quad + \sqrt{\eta}(\hat{a}_{\mathrm{LG}}(\omega)e^{-i\theta'} + \hat{a}_{\mathrm{LG}}(-\omega)^{\dagger}e^{i\theta'}),\end{aligned} \tag{8}$$

where $\hat{a}(\omega) = \int_{-\infty}^{+\infty}\hat{a}(t)e^{-i\omega t}\mathrm{d}t$, one has [23]

$$\begin{aligned}\langle|\hat{X}'_{s,\theta,\theta'}(\omega)|^2\rangle &= (1-\eta)\langle|\hat{X}_{s,\theta}(\omega)|^2\rangle \\ &\quad + \eta\langle\hat{a}_{\mathrm{LG}}(\omega)^{\dagger}\hat{a}_{\mathrm{LG}}(\omega) + \hat{a}_{\mathrm{LG}}(-\omega)^{\dagger}\hat{a}_{\mathrm{LG}}(-\omega) + 1\rangle \\ &= (1-\eta)\langle|\hat{X}_{s,\theta}(\omega)|^2\rangle \\ &\quad + \eta(\bar{n}_{\mathrm{LG}}(\omega) + \bar{n}_{\mathrm{LG}}(-\omega) + 1),\end{aligned} \tag{9}$$

where $\eta\bar{n}_{\mathrm{LG}}(\omega)$ and $\eta\bar{n}_{\mathrm{LG}}(-\omega)$ are the average photon numbers of the scattering field at frequencies $+\omega$ and $-\omega$. We assume $1/T_0 \geq 10^9$ Hz, i.e., $1/T_0$ is larger than the bandwidth of the depolarized GAWBS. In this case, substituting Eq. (9) into Eq. (7), one has

$$\langle\hat{X}'^2_{s,\theta,\theta'}\rangle = \langle\hat{X}^2_{s,\theta}\rangle + \eta\bar{n}_L + \eta, \tag{10}$$

where $\langle\hat{X}^2_{s,\theta}\rangle = (1-\eta)(T_0/2\pi)\int_{-\infty}^{+\infty}\langle|\hat{X}_{s,\theta}(\omega)|^2\rangle\mathrm{Sinc}^2(\omega T_0/2)\mathrm{d}\omega$, and $\bar{n}_L$ is the average photon number per pulsed LO. From Eq. (3), considering the fact that $\eta \ll 1$, the added excess noise can be given by

$$\langle\hat{X}^2_{\mathrm{LG},\theta}\rangle = \langle\hat{X}'^2_{s,\theta}\rangle - \langle\hat{X}^2_{s,\theta}\rangle \approx \eta\bar{n}_L. \tag{11}$$

Equation (11) shows that the added excess noise is equal to the average scattering photon number of the LO. In the above analysis, the single-mode fiber is assumed to be lossless. When considering the influence of the fiber loss, the scattering photon number at the fiber output can be given by

$$\bar{n}_{\mathrm{LG}} = \eta_1\bar{n}_L\int_0^l e^{-\alpha z}e^{-(l-z)\alpha}\mathrm{d}z = \eta_1 l e^{-\alpha l}\bar{n}_L, \tag{12}$$

where η_1 is the scattering efficiency due to the depolarized GAWBS per kilometer of fiber, and l and α are the length and loss coefficient of the fiber. From Eq. (12) it is evident that $\bar{n}_{\mathrm{LG}}$ is not a simple linear function of l due to the loss of the fiber. Intuitively, longer fiber can scatter more photons; however, the losses also increase accordingly, which results in the attenuation of both the LO and the scattering light. Figure 1(a) shows the modified scattering efficiency $\bar{n}_{\mathrm{LG}}/\bar{n}_L = \eta_1 l e^{-\alpha l}$ in units of η_1 as a function of fiber length. It is evident that the scattering efficiency increases with the length of the fiber at first and then reaches a maximum value of $8.17\eta_1$ at $l = 22$ km. Further increase of the fiber length will result in a lower scattering photon number at the fiber output due to the above-mentioned reasons.

In CVQKD, the excess noise of the quantum channel is referred to the channel input [6]; in such a case, Eq. (12) should be modified to

$$\bar{n}'_{\mathrm{LG}} = \bar{n}_{\mathrm{LG}}/e^{-\alpha l} = \eta_1 l\bar{n}_L, \tag{13}$$

where $\bar{n}'_{\mathrm{LG}}$ is the virtual scattering photon number, which is proportional to the fiber length [Fig. 1(b)].

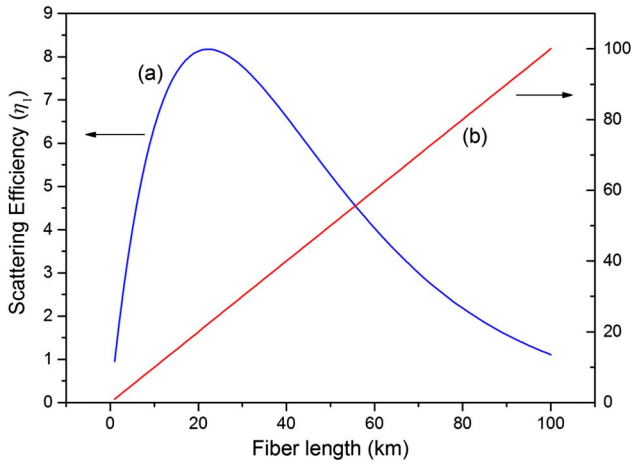

Fig. 1. Scattering efficiency versus fiber length when considering the fiber loss. (a) Actual scattering at the fiber output port. (b) Virtual scattering (see the text for details).

3. EXPERIMENTAL SETUP AND RESULTS

Figure 2 shows the experimental setup for measuring the depolarized GAWBS noise spectrum of SMF-28e. All optical components are fiber pigtailed. A 1550 nm single frequency linearly polarized continuous wave fiber laser is utilized. The polarization state of input light is adjusted such that the output laser from the SMF-28e single-mode fiber is also linear polarization. At the output port of the single-mode fiber, a polarizing beamsplitter (PBS) is used to separate the depolarized scattering light from the main transmitted light. The transmitted light (acting as a LO) combines again with the scattering light at a 50/50 beamsplitter (with the same polarization) for shot-noise-limited balanced homodyne detection. The relative phase between the LO and the scattering light can be varied by the phase modulator (PM). The subtracted photocurrent is amplified and input into an electronic spectrum analyzer.

Figure 3 shows a typical depolarized GAWBS spectrum for a 5 km long single-mode fiber SMF-28e (the core diameter is 125 μm, and the coating diameter is 245 μm). The input continuous wave power of the 1550 nm laser is 3 mW. When the relative phase between the LO and the scattering light is varied more than 2π, the measured noise spectrum remains almost unchanged and no evident variations can be seen, which is consistent with the results of Eq. (9) (here the input signal field $\hat{a}_s(t)$ is in a vacuum field). More than 30 depolarized GAWBS modes can be clearly seen with a typical

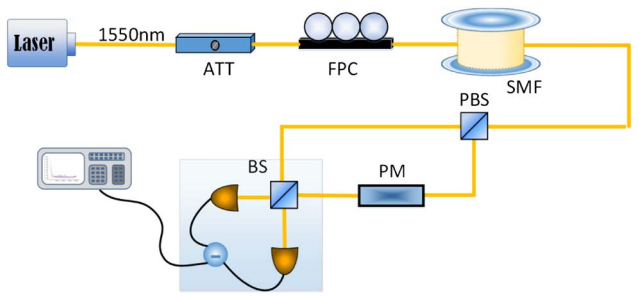

Fig. 2. Experimental setup for measuring the depolarized GAWBS noise spectrum. ATT, attenuator; FPC, fiber polarization controller; SMF, SMF-28e single-mode fiber; PBS, polarizing beamsplitter; PM, phase modulator; BS, 50/50 beamsplitter.

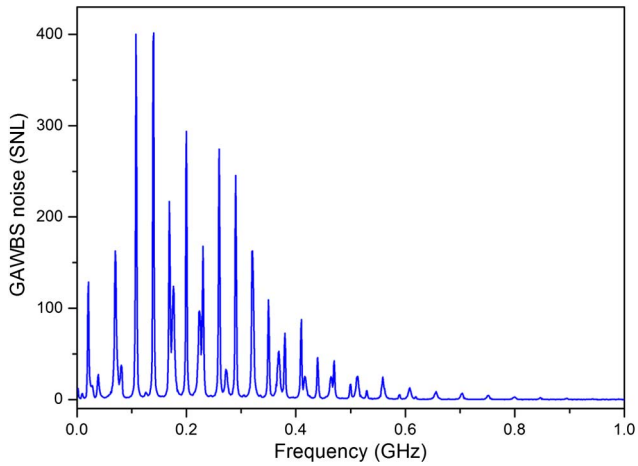

Fig. 3. Measured depolarized GAWBS spectrum with 3 mW 1550 nm input power in a 5 km SMF-28e single-mode fiber. The noise power is normalized to the shot-noise limit (SNL). Settings of the spectrum analyzer: resolution bandwidth is 300 kHz, and video bandwidth is 100 Hz.

linewidth of several megahertz for each scattering mode and overall bandwidth of around 600 MHz. To facilitate the comparison between the experiment and theory, the spectrum in Fig. 3 has been normalized to the shot-noise limit (SNL).

Figure 4 provides the GAWBS mode frequencies and the corresponding scattering efficiency. The circles are experimental results. Following from Eq. (9), each mode curve in Fig. 3 is integrated, and the obtained area, which is equal to the scattering photon number, is then divided by the LO photon number to give the scattering efficiency. The theoretical scattering efficiency [16] can be calculated by considering the radial and azimuthal strain at the fiber core and the strain-optic coefficients of fused silica (squares in Fig. 4). Good agreement was found for the measured and the calculated scattering mode frequencies. The measured scattering efficiencies agree roughly with the theoretical fittings. The first reason is that the silica optical fiber is surrounded by a polymer jacket (acrylate for SMF-28e), so coupling of acoustic radiation from the silica into the coated polymer will result in a mode-selective attenuation of the guided acoustic waves [24].

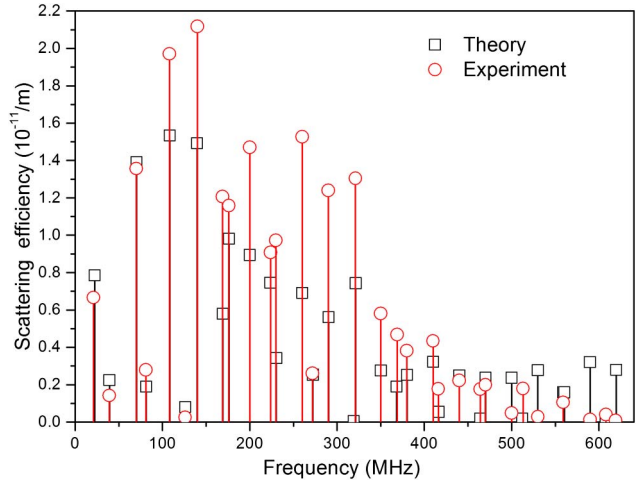

Fig. 4. Comparison of the mode frequencies and scattering efficiency between theory and experiment. The squares are the theoretical calculations, and the circles are the experimental results.

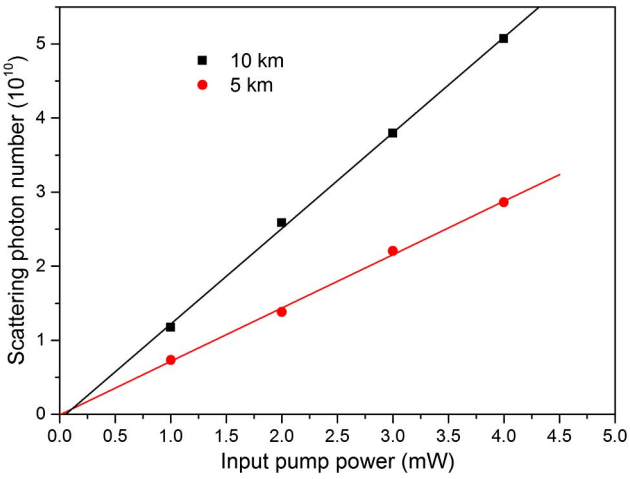

Fig. 5. Total scattering photon number over the frequency bandwidth of 1 GHz at different input optical powers. The squares and circles are experimental value for 5 km fiber and 10 km fiber, respectively. The solid lines are the linear fittings.

Another possible reason for such discrepancy is that the 5 km fiber is wound on a spool; interaction of the vibrational modes may exist among different parts of the fiber through the fiber surfaces, and this will further increase or decrease the scattering efficiencies for different vibrational modes.

Figure 5 shows the total scattering photon number over the frequency range from 2 MHz to 1 GHz as a function of input optical powers. Two fibers with different lengths (5 and 10 km) are investigated. Given the fiber length, the scattering photon number is proportional to the input optical power, which is consistent with Eq. (12). The slope ratio of the solid lines in Fig. 5 reflects the corresponding scattering efficiency for 5 and 10 km fibers, respectively. From Eq. (12), their scaling factor can be calculated as $10e^{-10\alpha}/(5e^{-5\alpha}) \approx 1.6$, which is in rough agreement with the measured value of 1.79; here the attenuation coefficient of the fiber used is $\alpha = 1\text{–}10^{-0.02}$, which is according to the nominal value of 0.2 dB/km.

4. DISCUSSION

From Eq. (12) and using the experimental results of Fig. 5, we can determine the scattering efficiency per kilometer of fiber to be $\eta_1 = 2.55 \times 10^{-7}$. By substituting η_1 into Eq. (13), one can obtain the virtual scattering photon numbers $\bar{n}'_{\mathrm{LG}}$, which is also equal to the added excess noise in CVQKD, as we have shown in Eq. (11). We assume that the CVQKD employs a time-multiplexing and polarization-multiplexing protocol in which a pulsed light with pulsewidth of 1 ns is utilized. Further taking $l = 100$ km, $\bar{n}_L = 10^8$, one has $\bar{n}'_{\mathrm{LG}} = 2.55 \times 10^3/h_E^G$, where h_E^G is the extinction ratio of the optical pulse. In general, to achieve a secure long-distance coherent state CVQKD, the excess noise should be controlled to be less than 1% of SNL [12]; this requirement will result in an extinction ratio of $h_E^G > 2.6 \times 10^5$. One should note that polarization multiplexing is not useful here to suppress this type of excess noise due to the depolarized scattering process.

It is useful to compare the extinction ratio requirement due to the depolarized GAWBS with that coming from LO leakage into the signal path. It has been shown [7] that the added excess noise due to the latter process can be given by $N_{\mathrm{leak}} = 2\langle n_{le}^e \rangle$, where $\langle n_{le}^e \rangle$ is the average photon number of the leakage, which is in the same spatiotemporal mode as the LO. It should be noted that this result is deduced based on the assumption that large unbalanced paths are employed to introduce a time delay between the LO and the signal field, and thus the relative phase ϕ_{le} between the LO and the leakage mode varies randomly in the range of 0–2π. For the high-bandwidth CVQKD considered here in which a narrow optical pulse (order of 1 ns) and a high pulse repetition rate (GHz) are employed, the LO and the signal paths are nearly balanced with a difference of only $\tau c/n \approx 10^{-9} \times 3 \times 10^8/1.5 \approx 0.2$ m. In this situation, the relative phase ϕ_{le} will drift with time slowly and the typical phase drifts are on the order of 10^{-3} per 0.1 s [7]. Hence the LO leakage will constitute mainly a constant background over the measured signal and can be subtracted. The residual fluctuations of the relative phase ϕ_{le} will introduce excess noise as $N_{\mathrm{leak}} = 4\bar{n}_{le}^e \langle (\Delta\phi_{le})^2 \rangle$, where $\bar{n}_{le}^e = \bar{n}_L/(h_p^L h_E^L)$, h_p^L is the polarization extinction ratio, and h_E^L is the temporal extinction ratio. Taking $N_{\mathrm{leak}} < 0.01$, $h_p^L = 10^3$, $\bar{n}_L = 10^8$, and $\langle (\Delta\phi_{le})^2 \rangle = 10^{-6}$ (0.1 s), one has $h_E^L > 4 \times 10^2$ for a perfect phase locking. Considering a more realistic locking precision of $\langle (\Delta\phi_{le})^2 \rangle = 10^{-4}$, one has $h_E^L > 4 \times 10^4$, which is smaller than h_E^G. This result denotes that the extinction ratio requirement due to the depolarized GAWBS is more critical than that coming from LO leakage into the signal path for a high-bandwidth (GHz) and long-distance (100 km) QKD.

5. CONCLUSIONS

In conclusion, we have investigated the effect of depolarized GAWBS in single-mode fibers on the excess noise in fiber-based CVQKD and show that the added excess noise is determined by the average scattering photon number of the LO. Based on the depolarized GAWBS spectrum measurement and analysis at various pump powers and fiber lengths, the scattering efficiency of SMF-28e is obtained. Then we calculate the lower bound for the extinction ratio of the pulsed light in the time-multiplexing CVQKD protocol, where 1% SNL unit excess noise is reached. The presented results will be useful to the design of a high-speed (GHz) CVQKD system in which the depolarized GAWBS noise will be nontrivial and relevant to the excess noise.

ACKNOWLEDGMENTS

This research is supported by the National Natural Science Foundation of China (NSFC) (11074156 and 61378010), the National Key Basic Research Program of China (2010CB923101), the NSFC Project for Excellent Research Team (61121064), and the Natural Science Foundation of Shanxi Province (2014011007-1).

REFERENCES

1. C. H. Bennett and G. Brassard, "Quantum cryptography: public key distribution and coin tossing," in *Proceedings of the IEEE International Conference on Computers, Systems and Signal Processing* (IEEE, 1984), pp. 175–179.
2. N. Gisin, G. Ribordy, W. Tittel, and H. Zbinden, "Quantum cryptography," Rev. Mod. Phys. **74**, 145–195 (2002).
3. V. Scarani, H. B. Pasquinucci, N. J. Cerf, M. Dušek, N. Lütkenhaus, and M. Peev, "The security of practical quantum key distribution," Rev. Mod. Phys. **81**, 1301–1350 (2009).
4. F. Grosshans, G. V. Assche, J. Wenger, R. Brouri, N. J. Cerf, and P. Grangier, "Quantum key distribution using Gaussian-modulated coherent states," Nature **421**, 238–241 (2003).
5. A. M. Lance, T. Symul, V. Sharma, C. Weedbrook, T. C. Ralph, and P. K. Lam, "No-switching quantum key distribution using

broadband modulated coherent light," Phys. Rev. Lett. **95**, 180503 (2005).
6. J. Lodewyck, M. Bloch, R. Garcia-Patron, S. Fossier, E. Karpov, E. Diamanti, T. Debuisschert, N. J. Cerf, R. Tualle-Brouri, S. W. McLaughlin, and P. Grangier, "Quantum key distribution over 25 km with an all-fiber continuous-variable system," Phys. Rev. A **76**, 042305 (2007).
7. B. Qi, L. L. Huang, L. Qian, and H. K. Lo, "Experimental study on the Gaussian-modulated coherent-state quantum key distribution over standard telecommunication fibers," Phys. Rev. A **76**, 052323 (2007).
8. Q. D. Xuan, Z. S. Zhang, and P. L. Voss, "A 24 km fiber-based discretely signaled continuous variable quantum key distribution system," Opt. Express **17**, 24244–24249 (2009).
9. P. Jouguet, S. K. Jacques, T. Debuisschert, S. Fossier, E. Diamanti, R. Alléaume, R. T. Brouri, P. Grangier, A. Leverrier, P. Pache, and P. Painchault, "Field test of classical symmetric encryption with continuous variables quantum key distribution," Opt. Express **20**, 14030–14041 (2012).
10. L. S. Madsen, V. C. Usenko, M. Lassen, R. Filip, and U. L. Andersen, "Continuous variable quantum key distribution with modulated entangled states," Nat. Commun. **3**, 1083 (2012).
11. P. Jouguet, S. K. Jacques, A. Leverrier, P. Grangier, and E. Diamanti, "Experimental demonstration of long-distance continuous-variable quantum key distribution," Nat. Photonics **7**, 378–381 (2013).
12. I. Khan, C. Wittmann, N. Jain, N. Killoran, N. Lütkenhaus, C. Marquardt, and G. Leuchs, "Optimal working points for continuous-variable quantum channels," Phys. Rev. A **88**, 010302(R) (2013).
13. W. C. Dai, Y. Lu, J. Zhu, and G. H. Zeng, "An integrated quantum secure communication system," Sci. China Inf. Sci. **54**, 2578–2591 (2011).
14. X. Y. Wang, Z. L. Bai, S. F. Wang, Y. M. Li, and K. C. Peng, "Four-state modulation continuous variable quantum key distribution over a 30-km fiber and analysis of excess noise," Chin. Phys. Lett. **30**, 010305 (2013).
15. P. Jouguet, S. K. Jacques, and A. Leverrier, "Long-distance continuous-variable quantum key distribution with a Gaussian modulation," Phys. Rev. A **84**, 062317 (2011).
16. R. M. Shelby, M. D. Levenson, and P. W. Bayer, "Resolved forward Brillouin scattering in optical fiber," Phys. Rev. Lett. **54**, 939–942 (1985).
17. R. M. Shelby, M. D. Levenson, and P. W. Bayer, "Guided acoustic-wave Brillouin scattering," Phys. Rev. B **31**, 5244–5252 (1985).
18. K. Bergman and H. A. Haus, "Squeezing in fibers with optical pulses," Opt. Lett. **16**, 663–665 (1991).
19. R. M. Shelby, M. D. Levenson, S. H. Perlmutter, R. G. Devoe, and D. F. Walls, "Broad-band parametric deamplification of quantum noise in an optical fiber," Phys. Rev. Lett. **57**, 691–694 (1986).
20. M. D. Levenson, R. M. Shelby, A. Aspect, M. Reid, and D. F. Walls, "Generation and detection of squeezed states of light by nondegenerate four-wave mixing in an optical fiber," Phys. Rev. A **32**, 1550–1562 (1985).
21. M. Rosenbluh and R. M. Shelby, "Squeezed optical solitons," Phys. Rev. Lett. **66**, 153–156 (1991).
22. J. F. Corney, P. D. Drummond, J. Heersink, V. Josse, G. Leuchs, and U. L. Andersen, "Many-body quantum dynamics of polarization squeezing in optical fibers," Phys. Rev. Lett. **97**, 023606 (2006).
23. J. G. Webb, T. C. Ralph, and E. H. Huntington, "Homodyne measurement of the average photon number," Phys. Rev. A **73**, 033808 (2006).
24. A. J. Poustie, "Bandwidth and mode intensities of guided acoustic-wave Brillouin scattering in optical fibers," J. Opt. Soc. Am. B **10**, 691–696 (1993).